

# Inactivation of V79 cells by low-energy protons, deuterons and helium-3 ions

M. FOLKARD\*, K.M. PRISE, B. VOJNOVIC, H.C. NEWMAN, M.J. ROPER and B.D. MICHAEL

(Received 19 December 1995; revision received 23 February 1996; accepted 5 March 1996)

**Abstract.** Previous work by ourselves and by others has demonstrated that protons with a linear energy transfer (*LET*) about  $30 \text{ keV}\mu\text{m}^{-1}$  are more effective at killing cells than doubly charged particles of the same *LET*. In this work we show that by using deuterons, which have about twice the range of protons with the same *LET*, it is possible to extend measurements of the *RBE* of singly charged particles to higher *LET* (up to  $50 \text{ keV}\mu\text{m}^{-1}$ ). We report the design and use of a new arrangement for irradiating V79 mammalian cells. Cell survival measurements have been made using protons in the energy range 1.0–3.7 MeV, deuterons in the energy range 0.9–3.4 MeV and  $^3\text{He}^{2+}$  ions in the energy range 3.4–6.9 MeV. This corresponds to volume-averaged *LET* (within the cell nucleus) between 10 and  $28 \text{ keV}\mu\text{m}^{-1}$  for protons,  $18\text{--}50 \text{ keV}\mu\text{m}^{-1}$  for deuterons, and  $59\text{--}106 \text{ keV}\mu\text{m}^{-1}$  for helium ions. Our results show no difference in the effectiveness of protons and deuterons matched for *LET*. However, for *LET* above about  $30 \text{ keV}\mu\text{m}^{-1}$  singly charged particles are more effective at inactivating cells than doubly-charged particles of the same *LET* and that this difference can be understood in terms of the radial dose distribution around the primary ion track.

## 1. Introduction

Studies related to the fundamental mechanisms of radiation action seek to understand the spatial qualities of ionizing radiation that determine its effect on tissue. It is now widely believed that it is the extent to which ionizations are clustered over nanometre distances that determines radiation effect (Frankenberg *et al.* 1986, Thacker *et al.* 1986, Goodhead 1994). The relationship between clustering of ionizations, the subsequent complexity of the DNA lesion produced and the eventual radiobiological effect, has so far largely been the domain of track-structure modelling studies. Low-energy light ions can have radiobiological properties associated with both sparsely and densely ionizing radiations, depending upon their energy, and therefore provide an

experimental opportunity for investigating the role of ionization density. Studies using low-energy singly charged particles are also of importance to understanding the risk associated with environmental and occupational exposures to fast neutrons where much of the damage is due to low-energy recoil protons. Also, there is increasing interest in the use of protons in radio-surgery and radiotherapy (Raju 1995). We have previously reported experiments measuring the relative biological effectiveness (*RBE*) for cell survival (Folkard *et al.* 1989), and DNA damage (Prise *et al.* 1990) using protons with selected energies  $<2 \text{ MeV}$ . Our findings from these initial studies were that for protons with *LET*  $>17 \text{ keV}\mu\text{m}^{-1}$ , the *RBE* for inactivating V79 mammalian cells increases with increasing *LET* and that protons with an *LET* of about  $30 \text{ keV}\mu\text{m}^{-1}$  were more effective than earlier data had shown for doubly charged particles of the same *LET*. Similar results regarding the increased effectiveness of protons have been reported by Belli *et al.* (1993) who have studied the inactivation of V79 cells and by Goodhead *et al.* (1992) and Belli *et al.* (1992a) who have studied both the inactivation of V79, HeLa and C3H 10T<sup>1/2</sup> cells and the mutation of V79 cells by low-energy protons and  $\alpha$ -particles. The observed differences in the lethality of protons and  $\alpha$ -particles with the same *LET* highlights the importance of track-structure (as distinct from ionization density along the track) in determining the biological effect of a radiation. Protons and  $\alpha$ -particles which have the same ionization density along the primary ion track (i.e. the same *LET*) nevertheless differ in respect of the distribution of dose around the track.

Little reliable data so far exists for the effectiveness of protons with *LET* values greater than about  $30 \text{ keV}\mu\text{m}^{-1}$ . The data of Belli *et al.* (1993) includes measurements for the *RBE* of protons with *LET* values of 64 and  $89 \text{ keV}\mu\text{m}^{-1}$ . These *LET* values are however, a re-evaluation of

\*Author for correspondence.

Gray Laboratory Cancer Research Trust, PO Box 100, Mount Vernon Hospital, Northwood HA6 2JR, UK.

earlier work (Belli *et al.* 1989, 1992b) and the authors indicate that these two data points are now unreliable. A difficulty of experimenting with protons which have  $LET > 30 \text{ keV}\mu\text{m}^{-1}$  is that the range of the proton in tissue is not much greater than the diameter of a mammalian cell. Also, as the proton  $LET$  is increased, the spread of  $LET$  within the nucleus becomes large and track-segment conditions no longer apply. Furthermore, it is difficult to estimate reliably the average  $LET$ , as small deviations from the idealized experimental arrangement can significantly affect this quantity. To overcome this limitation, we have performed experiments using deuterons as well as protons. Deuterons with the same  $LET$  as protons also have the same velocity and track-structure and therefore (presumably) similar radiobiological properties. However, the range of the deuterons is roughly twice that of protons of the same  $LET$ , and the corresponding spread of  $LET$  within the nucleus is less. By using deuterons, we have been able to extend our measurements of the  $RBE$  for inactivation by singly charged particles to higher  $LET$ . We have further improved the reliability of measurements made at higher  $LET$  by re-designing the experimental arrangement to reduce, as far as possible, the energy lost by particles reaching the cells. This development minimises the energy spread incident at the cell surface, and also allows us to use  ${}^3\text{He}^{2+}$  ions with sufficient energy, such that their  $LET$  is comparable with that obtained using singly charged particles.

We have also investigated the  $RBE$  of deuterons with higher energies, so that their effect can be compared with protons at lower  $LET$  to confirm that the  $RBE$  values for  $LET$ -matched protons and deuterons are the same. We have given this aspect of the study particular attention following a reported difference in the  $RBE$  of proton and deuterons with the same  $LET$ , both for cell inactivation (Belli *et al.* 1994) and mutation (Cherubini *et al.* 1993).

In this paper, we describe the design, construction and dosimetry of our new arrangement for irradiating V79 mammalian cells using low-energy protons in the energy range 1.0–3.7 MeV, deuterons in the energy range 0.9–3.4 MeV and helium ions in the energy range 3.4–6.9 MeV. This corresponds to volume-averaged  $LET$  (within the cell nucleus) between 10 and  $28 \text{ keV}\mu\text{m}^{-1}$  for protons,  $18$ – $50 \text{ keV}\mu\text{m}^{-1}$  for deuterons and  $59$ – $106 \text{ keV}\mu\text{m}^{-1}$  for helium ions. Our results suggest that at moderate  $LET$  (about  $40$ – $50 \text{ keV}\mu\text{m}^{-1}$ ), singly-charged particles are more effective at

inactivating cells than doubly charged particles with similar  $LET$ . We also find no difference in the effectiveness of protons and deuterons matched for  $LET$ .

## 2. Materials and methods

### 2.1. Experimental arrangement

Energetic particles are produced using the Gray Laboratory Van de Graaff accelerator. This is nominally rated to operate at an accelerating voltage of 4MV, but in practice will operate stably at any selected value between about 2 and 4.2MV. An analyzing magnet that bends the beam through  $90^\circ$  is used to select accelerated particles of the required type and energy so that near-monoenergetic particles are delivered to the sample, at the end of a horizontal beamline about 6m from this magnet. The usual complement of electrostatic deflectors and quadrupole magnets are available to steer and shape the beam.

An arrangement for irradiating cells has been reported previously (Folkard *et al.* 1989), however this underwent partial modification (Folkard *et al.* 1995) and then further extensive modification for the current study. The current modifications have been designed to reduce as far as possible the energy lost by the particles reaching the cell surface. This is beneficial for several reasons; first, the reproducibility of the energy at the sample position with successive experiments is now much improved. Second, the energy-spread at the sample position due to straggling is reduced. Finally, it extends the range of energies that can be studied and allows us to use  ${}^3\text{He}^{2+}$  ions with which very little energy loss can be tolerated if we are to approach the  $LET$  possible for singly-charged particles. Although it is possible to accelerate  ${}^4\text{He}^{2+}$  ions, the maximum accelerating potential available does not allow us to achieve a condition where we could match the  $LET$  of  ${}^4\text{He}^{2+}$  to that of deuterons. Note that some data have been incorporated in this study from the partially modified version, which gave similar results to the current version (where  $LET$  values could be matched).

The new arrangement is illustrated in figure 1a and b. Up to 12 samples are supported on a 29 cm diameter rotating aluminium platter that sweeps each sample once through the radiation field. The speed of rotation (and hence the dose) can be accurately and independently preset for each

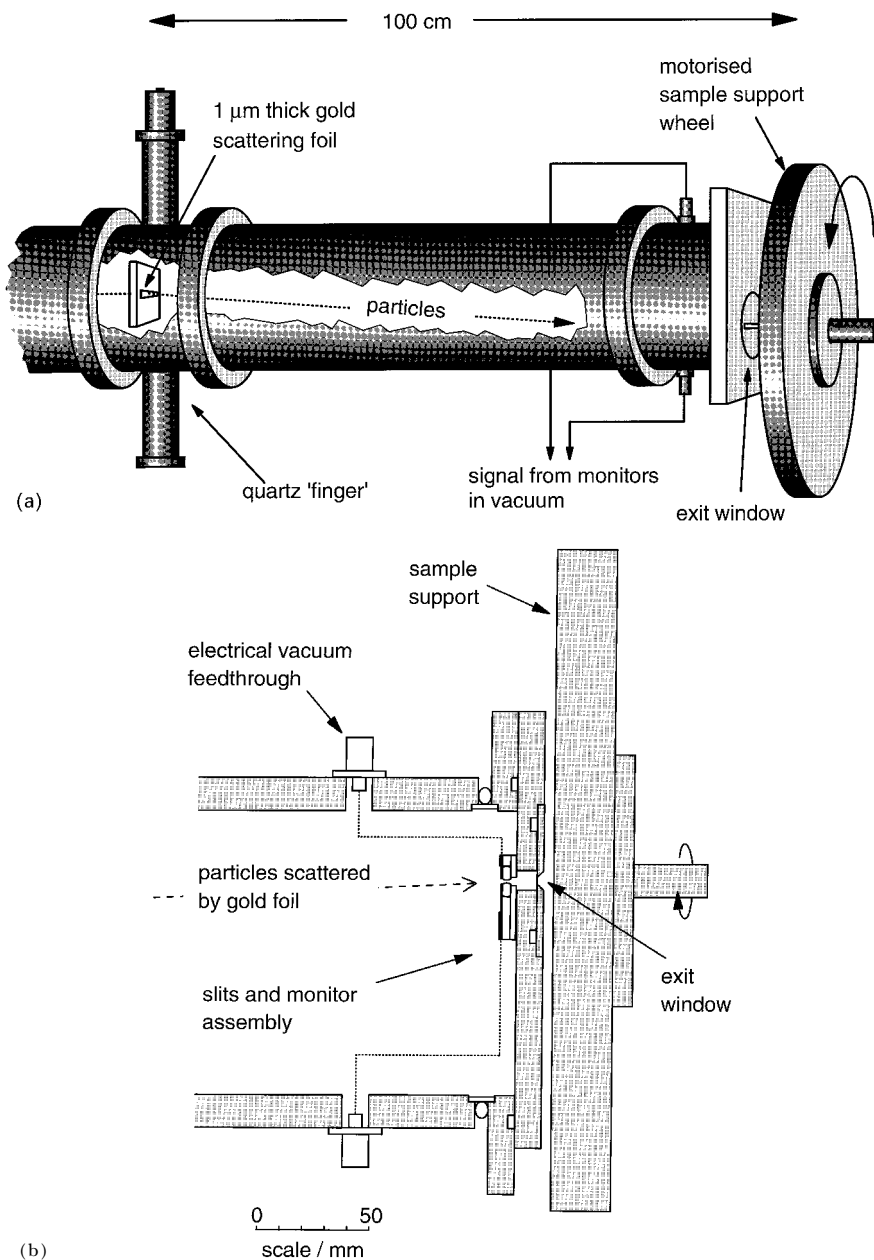


Figure 1. (a) Overall and (b) plan views of the sample irradiation apparatus.

sample. The exit window of the beamline is made from either 13 μm, or 25 μm thick polyimide (Kapton, Du Pont) film, supported by a vacuum-tight flange over a 3 × 26 mm vertical slit. The window is recessed 2 mm into the end-face of the beamline and this distance represents the smallest window-to-sample gap that can be achieved. A slit that defines the shape of the field is mounted just before the exit window (i.e. in the vacuum). The edges of the slit are machined from 5 mm diameter steel rod and define a near-rectangular field (the edges are aligned with radii of the rotating platter and are therefore not parallel) about 1 × 26 mm.

Mounted to the slit are four (two per slit) 12 × 4 mm charge-collecting plates, sandwiched between 20 μm thick mica for electrical isolation and each connected by insulated wire to an electrical vacuum feedthrough. These serve to monitor the dose to the sample and although the four plates operate independently, it has been found sufficient to simply sum and then measure the charges on a single electrometer. A position sensor on the wheel provides a signal that 'enables' this electrometer, such that charge is integrated only when the sample is crossing the field. Additionally, a continuous analogue and

digital readout of the current from the monitor is displayed. These are used to check (and if necessary adjust) the dose-rate before each sample is irradiated, and to verify that the dose-rate does not change during the irradiation (which would cause the dose to vary across the sample).

A 1  $\mu\text{m}$  thick gold scattering foil is mounted 1m from the exit window in the vacuum. The scattering area is reduced to 1  $\times$  30 mm by a slit similar to that mounted near the exit window. The window-slit-monitor assembly can be positioned up to 30 mm horizontally off-axis, so that only particles scattered by the gold foil can pass through the exit window. A quartz disk can be inserted into the path of the beam close to the gold foil. The fluorescence due to incident accelerated particles striking the quartz can be viewed remotely through a vacuum window and is used at the beginning of each session to ensure that the beam is spread evenly over the scattering foil. A further check is made by using an integrating electronic camera to view the fluorescence induced in a quartz slide temporarily fixed over the exit window. The image is processed and viewed using a 486-personal computer which enables the dose distribution across the exit window to be readily evaluated. By using a scattering foil, a uniform dose distribution can be achieved over the portion of the beam to which the cells are exposed.

## 2.2. Dose and energy measurement

The methods for measuring the dose and energy at the sample position have been described in detail elsewhere (Folkard *et al.* 1989). A parallel-plate extrapolation chamber is used to measure the dose at the sample position and thus calibrate the monitor. Particles enter the chamber cavity through the polarizing electrode, which is made from 3  $\mu\text{m}$  thick aluminized Mylar. The other electrode is a 13 mm diameter copper plate surrounded by a guard-ring and the gap between this and the polarizing electrode can be accurately adjusted down to 0.3 mm. The chamber can be mounted in place of the rotating sample platter at the appropriate distance from the window such that it can be swept through the particle beam at a precise angular velocity. The total electric charge accumulated by the chamber during one sweep is measured using an electrometer (Keithley, type 616) and by repeating the process for a number of plate spacings,  $x$ , the charge,  $Q$ , per unit plate spacing,  $dQ/dx$ , can be ascertained. The dose,  $D$ ,

can be calculated using the following expression,

$$D = \frac{W}{eA\rho_a} \frac{(\mu/\rho)_s}{(\mu/\rho)_a} k_{\text{tp}} \frac{dQ}{dx} \quad (1)$$

where  $W/e$  is the average energy per ion pair for singly charged protons and deuterons or doubly-charged  $^3\text{He}^{2+}$  ions (35  $\text{J C}^{-1}$  was used throughout),  $A$  is the area of the collecting electrode (136  $\text{mm}^2$ ),  $\rho_a$  is the density of air at STP,  $k_{\text{tp}}$  is a temperature and pressure correction factor, and  $(\mu/\rho)_s/(\mu/\rho)_a$  is the ratio of stopping powers of the sample and air. A value of 1.15–1.17 (depending on the particle and its energy) was used, derived from the stopping power data for liquid water and dry air (protons and  $\alpha$ -particles), tabulated in ICRU (1993).

To measure the energy at the sample position, a ruggedized silicon surface-barrier detector was used (EG & G Ortec, 300  $\mu\text{m}$  depletion depth) in conjunction with conventional spectroscopy electronics. The detector was calibrated in vacuum using an unsealed  $^{241}\text{Am}$  isotope source. The detector is constructed such that the active region is recessed 4 mm into the mount. Since the vacuum window on the Van de Graaff beamline is recessed 2 mm, the minimum air path that can be achieved between the window and the detector is 6 mm. To enable energy (and dose) measurements to be made at the sample position, the window to sample distance was also set at 6 mm, although samples can be irradiated closer than this, if necessary.

## 2.3. Sample preparation

The particles of interest in this study have a short range, therefore it is necessary to support the cells as a monolayer. Chinese hamster V79-379A cells were maintained in Eagles minimal medium (EMEM) containing 10% foetal calf serum and antibiotics. A suspension of cells in exponential phase was concentrated to  $10^7 \text{ ml}^{-1}$  in Hepes-buffered EMEM and 20  $\mu\text{l}$  spread onto 13 mm diameter polyvinylidene difluoride filters (0.22  $\mu\text{m}$  pore size, Millipore Corp.). The filters rested on 1.0% (w/v) agar made up in cell culture medium. After a few minutes, the medium surrounding the cells soaked through the filter to leave an unattached monolayer of cells on the filter in contact with enough medium to keep the cells viable, but not enough to cause appreciable radiation shielding. The prepared filters have a matte appearance when this condition is

reached. The filter was then transferred to the irradiation platter where it was supported on moistened filter paper (Whatman No. 1) by surface tension. The platter was cooled to about  $10^{\circ}\text{C}$  below the ambient temperature to prevent the samples drying out. The cooling was achieved by circulating chilled antifreeze through a cavity within the platter. Cells were typically on the platter for  $<10$  min in ambient atmosphere. After irradiation, the cells were washed off the filters, counted, diluted and plated out. The plated cells were incubated for 6 days in an atmosphere of 95% air:5%  $\text{CO}_2$  after which, they were stained and colonies containing  $\geq 50$  cells were scored. At least three independent experiments were performed for each cell survival data point.

#### 2.4. X-irradiation

The X-irradiations were performed using 240 kVp X-rays. The cells were exposed on membrane filters as described in §2.3 at a dose-rate of  $1.6\text{ Gy min}^{-1}$ . A thick (5 mm) Perspex lid was placed over the cells to provide build-up. The irradiations took place with cells at  $4^{\circ}\text{C}$  in atmospheric air.

### 3. Results and discussion

#### 3.1. Energy measurements and LET evaluations

The particles crossing each cell will have a spread of *LET* within the nucleus. This spread is due both to the energy distribution of the incident particles and to the energy lost by each particle as it crosses the cell. It is possible to calculate the *LET* spectrum within the nucleus provided the incident energy spectrum and the shape of the cells and their nuclei are known. From the *LET* spectrum we can derive the volume-averaged *LET*, a single-value that can be assigned to any given experimental conditions. The measured mean energy and range of particles incident at the cell surface (6 mm window-to-sample distance) is summarised in table 1. In all cases, the full energy peak can be described by a simple Gaussian curve and very few particles are detected outside this peak. The measured full width at half maximum (FWHM) energy spread is between 80 and 140 keV in all cases except for the lowest energy proton data, which has a FWHM of 180 keV. This is because it was not possible to reduce the accelerator voltage sufficiently to

achieve the desired energy at the cell surface without the use of absorbers.

The shape of the cells while supported by the filter is assumed to be similar in appearance to that described by Datta *et al.* (1976) for studies of track-end  $\alpha$ -particles. They depict the cell as a 'flattened-sphere',  $10\ \mu\text{m}$  thick. This is clearly a simplification of the true conditions, where the cells have a range of shapes and sizes. Limited measurements made by us using a confocal microscope show that this is a reasonable representation for calculation purposes (Folkard *et al.*, unpublished data). These observations have been used to construct a three-dimensional computer-model of the cell and its nucleus (Folkard *et al.* 1989), from which we can calculate the LET spectrum (and hence, the volume-averaged LET) within the cell nucleus for all experimental arrangements. Energy losses within the cell were estimated using tabulated data for proton and  $\alpha$ -particle stopping powers in liquid water (ICRU 1993). Deuteron stopping powers were assumed to be those for protons at half the energy.  $^3\text{He}^{2+}$  ions are assigned stopping powers equivalent to those for  $\alpha$ -particles at four-thirds the energy. The calculated volume-averaged *LET* and the spread of *LET* within the cell nucleus are shown in figure 2 as a function of the incident mean energy. It is evident that we get the expected improvement (i.e. reduction) in the spread of *LET* when deuterons are used instead of protons of equivalent *LET*. The measurements performed

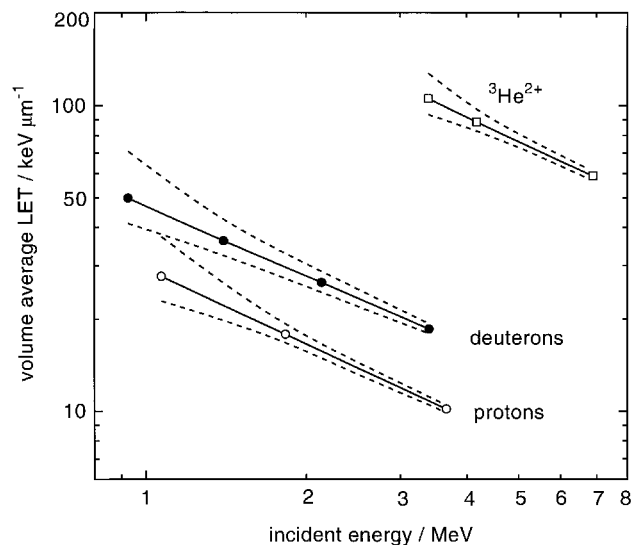


Figure 2. Calculated volume-averaged LET within the cell nucleus as a function of the mean incident energy. The dashed lines above and below each data set indicate the maximum and minimum LET present within the cell nucleus.

using higher energy particles reasonably resemble true track-segment experiments, as the *LET* is similar throughout the cell nucleus. At lower energies, the average *LET* within the nucleus and the spread of *LET* both increase. Above about  $25 \text{ keV } \mu\text{m}^{-1}$  for protons and  $40 \text{ keV } \mu\text{m}^{-1}$  for deuterons, the average *LET* is sensitive to small changes in both the incident energy and cell shape. Variability in the cell (and nucleus) thickness will affect the value of the maximum *LET* present within the nucleus, much more than the minimum value (which is affected only by the thickness of the cytoplasm). For example, using  $0.93 \text{ MeV}$  deuterons (which is the ‘worst-case’ regarding sensitivity to cell shape), a  $\pm 10\%$  uncertainty in cell nucleus thickness would mean that the uncertainty in the maximum *LET* within the nucleus is also about  $\pm 10\%$  in this instance. The corresponding uncertainty in the volume-averaged *LET* will be roughly half of this value (i.e. about  $\pm 5\%$ ). For other particles and energies, the uncertainty is less than this.

### 3.2. Measurements of cell survival

Figure 3a–c shows representative cell survival curves after irradiation with protons, deuterons,  ${}^3\text{He}^{2+}$  and for comparison, 240 kVp X-rays. The error-bars are  $\pm 1$  standard error. All the data are fitted using the linear-quadratic model such that the surviving fraction (*SF*) is described by the equation,

$$SF = \exp -(\alpha D + \beta D^2).$$

It is evident from both the proton and the deuteron data that as the energy of the incident particles is reduced (i.e. the average *LET* increased) the appearance of the survival curves change from low *LET* in character to high *LET*. That is, the curves become steeper and shoulder is reduced. For the highest *LET* deuteron data, the shoulder disappears completely. It can be seen that for both the highest proton and deuteron *LET* survival curves there is no evidence of a ‘tail’ or plateau at high doses, which might be seen if a fraction of the cells were shielded. At these energies, the range of the particles is not much greater than the width of the cell, therefore even a small amount of unwanted shielding, or ‘piling-up’ of cells would cause a plateau at relatively modest surviving fraction levels. There is an indication of shielding for the helium ion data and in this instance, the shielded data are not included in the curve-fits.

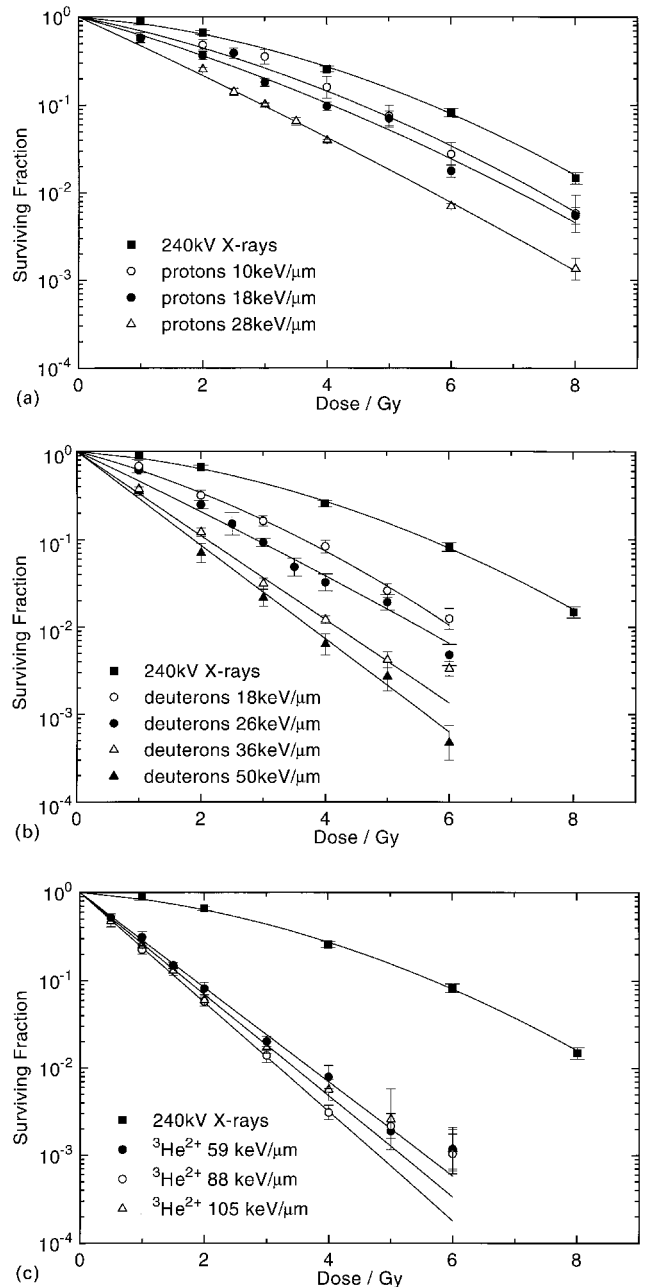


Figure 3. Surviving fraction of V79-379A cells after exposure to (a) protons, (b) deuterons, and (c)  ${}^3\text{He}^{2+}$  ions. The survival after exposure to 240 kVp X-rays is also depicted. The data are fitted by the method of least-squares using the linear-quadratic model. Error bars are  $\pm 1$  standard error.

The *RBE* at the 10% surviving fraction for all proton, deuteron and helium ion incident energies are plotted against volume-averaged *LET* in figure 4, and are tabulated along with other experimental parameters in table 1. Each *RBE* is the average of a minimum of three experiments and the error bars are derived from ‘worst-case’ fits to the particle and X-ray data, when the respective

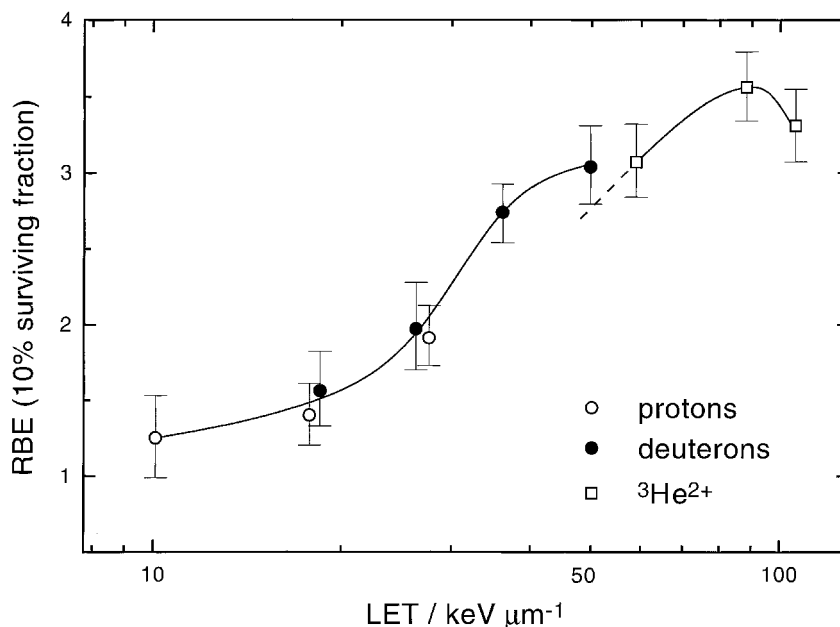


Figure 4. *RBE* at 10% surviving fraction for protons, deuterons and  ${}^3\text{He}^{2+}$  ions as a function of volume-averaged LET within the cell nucleus. The error bars are derived from 'worst-case' fits to the survival curves. The curves through the data are drawn by eye.

errors for  $\alpha$  and  $\beta$  are considered. The measured *RBE* of protons at around  $30 \text{ keV } \mu\text{m}^{-1}$  is less than our previous measurement (Folkard *et al.* 1989). In this study however, the spread of *LET* within the cell nucleus has been much reduced (in particular, there are fewer contaminating low-energy protons, which have higher *RBE*) and we believe our current result better reflects the *RBE* at this *LET*.

It can be seen that at all *LET* values used in this study, the effectiveness of singly-charged particles increases with increasing *LET*. It is evident that the same *RBE-LET* relationship can be used to describe the effects of both protons and deuterons. This result contrasts with a report by Belli *et al.* (1994) and a preliminary report by Cherubini *et al.* (1993) who find that

$<31 \text{ keV } \mu\text{m}^{-1}$  deuterons are less effective than protons with the same *LET* for cell survival. Their findings are unexpected as current physical descriptions indicate that the track structures of protons and deuterons are identical when the *LET* is the same. For singly charged particles, the trend of increasing *RBE* with *LET* begins to 'flatten-out' at the highest *LET* ( $49.8 \text{ keV } \mu\text{m}^{-1}$ ) such that a peak in effectiveness may exist around  $55\text{--}65 \text{ keV } \mu\text{m}^{-1}$ . The data for  ${}^3\text{He}^{2+}$  ions and  $\alpha$ -particles indicates a maximum *RBE* for doubly charged particles about  $90\text{--}100 \text{ keV } \mu\text{m}^{-1}$  in agreement with other studies (i.e. Thacker *et al.* 1979).

Despite the improvements to our irradiation apparatus, we have been unable to achieve a

Table 1. Incident energy, the range, the volume-averaged LET, values for  $\alpha$  and  $\beta$  from the linear-quadratic fits to the data and *RBE* (initial slopes and at 10% surviving fraction) for the particles used in this study.

Radiation	Incident energy (MeV)	CSDA range in water ( $\mu\text{M}$ )	LET ( $\text{KeV } \mu\text{m}^{-1}$ )	$\alpha$ ( $\text{Gy}^{-1}$ )	$\beta$ ( $\text{Gy}^{-2}$ )	<i>RBE</i> $\alpha/\alpha$ (X-ray)	<i>RBE</i> (10% <i>SF</i> )
X-rays	240 kVp			$0.13 \pm 0.022$	$0.048 \pm 0.003$	1.00	1.00
Protons	3.66	210	10.1	$0.32 \pm 0.058$	$0.039 \pm 0.011$	2.49	1.25
	1.83	65	17.8	$0.45 \pm 0.035$	$0.028 \pm 0.006$	3.42	1.40
	1.07	27	27.6	$0.74 \pm 0.025$	$0.011 \pm 0.004$	5.63	1.91
Deuterons	3.40	115	18.5	$0.43 \pm 0.050$	$0.055 \pm 0.009$	3.28	1.56
	2.14	55	26.3	$0.76 \pm 0.051$	$0.013 \pm 0.008$	5.77	1.97
	1.40	28	36.1	$1.10 \pm 0.014$	0.0	8.35	2.74
${}^3\text{He}^{2+}$	0.93	16	49.8	$1.23 \pm 0.033$	0.0	9.32	3.04
	6.90	74	58.9	$1.24 \pm 0.025$	0.0	9.41	3.07
	4.18	33	88.3	$1.44 \pm 0.008$	0.0	10.90	3.56
	3.39	24	105.8	$1.33 \pm 0.019$	0.0	10.11	3.31

condition where singly and doubly charged particles can be exactly matched for *LET*. Nevertheless, if lines drawn through the data are extrapolated slightly, then there is the suggestion that at moderate *LET* ( $30\text{--}50\text{ keV }\mu\text{m}^{-1}$ ), singly-charged particles are more effective than doubly-charged particles of the same *LET*. We do not expect that it will be possible to measure reliably the *RBE* for singly charged particles with *LET* much beyond about  $50\text{ keV }\mu\text{m}^{-1}$ , because the particle range will then be too short. Our highest *LET* data point for singly charged particles was obtained using deuterons with a mean incident energy of  $0.93\text{ MeV}$ , which corresponds to a range in the cell of about  $16\text{ }\mu\text{m}$ . To reduce the energy still further increases the risk that particles will be fully stopped within the cell. Another difficulty is that the spread of *LET* within the nucleus is large at high *LET* (figure 2) which makes interpretation of the data less straightforward. Clearly, the measured *RBE* corresponds to an average effect of the distribution of *LET* within the nucleus and is therefore not representative of a true track-segment experiment in this instance. One method of countering this problem is to use thinner or attached cells (which flatten) so that the particles have less cell thickness to traverse. Although the cells remain rounded using the method reported here, this has the advantage that it probably ensures a greater uniformity in the cell-to-cell exposure compared to an attached cell system. Belli *et al.* (1989) irradiate V79 cells

attached to  $52\text{ }\mu\text{m}$  thick Mylar (through the Mylar) and suggest that 'plateau' in their cell survival data could be caused by poorly attached or shielded cells, and also by the existence of a sub-population of rounded mitotic cells.

Where our data for protons and deuterons overlap with those of other workers using the same cell line as ourselves, there is broad agreement with their findings. This is evident in figure 5, where we have plotted our *RBE-LET* data alongside that of Perris *et al.* (1986) and Belli *et al.* (1993, 1994). In this instance the *RBE* is defined in terms of the ratio of the initial slopes of the proton (or deuteron) and X-ray survival curves (i.e.  $\alpha/\alpha_x$ ), in accordance with the method used in these papers. Our results agree well with the proton data of Perris *et al.* (1986) and with the proton data (but not, as explained earlier, the deuteron data) of Belli *et al.* (1993, 1994) up to  $30\text{ keV }\mu\text{m}^{-1}$ . Beyond this value, the data of Belli *et al.* shows the *RBE* of protons decreasing with increasing *LET*, although they state that their high *LET* data are unreliable, and therefore do not claim to have identified a maximum in the *RBE-LET* relationship.

It has been pointed out in previous studies using low-energy protons that the increased *RBE* of protons and deuterons compared with helium ions most likely reflects differences in the particle track-structure. Singly charged particles have a lower velocity than helium ions of the same *LET*, therefore the energy spectrum of the secondary

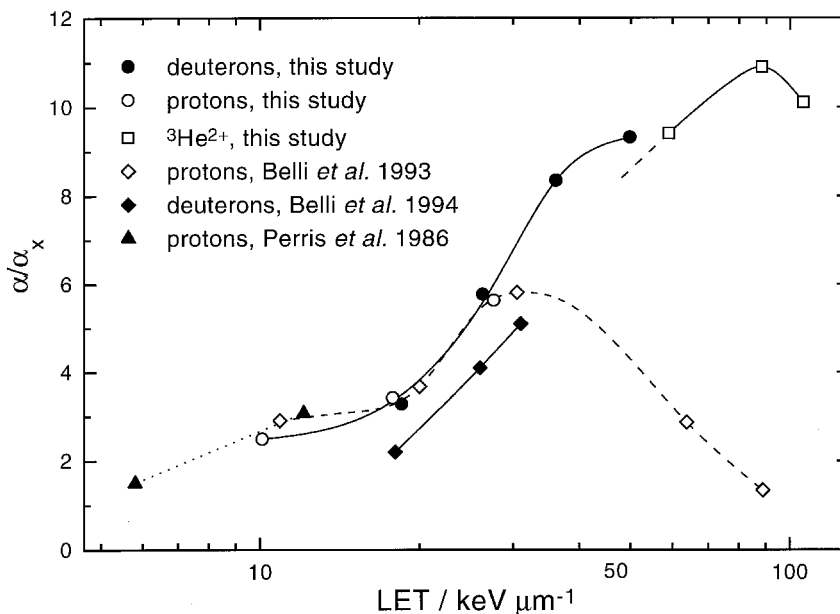


Figure 5. *RBE* derived from the initial slope of the survival curves ( $\alpha/\alpha_x$ ) as a function of volume-averaged *LET*. Also shown for comparison are the data of Belli *et al.* (1993, 1994) and Perris *et al.* (1986).

electrons is also reduced with the consequence that the ionizations produced by these electrons are more tightly clustered around the primary ion track. The increased lethality of protons and deuterons compared to helium ions is therefore consistent with models that place importance on the extent to which ionizations are clustered at the nanometer level (Goodhead 1994). Another point to note is that radiation protection monitoring methods that rely on microdosimetric measuring techniques cannot distinguish between singly and doubly charged particles with the same *LET*. This is particularly relevant to neutron fields where a significant fraction of the dose is due to low-energy proton recoils. If, as these data suggest, the energies of the secondary electrons are important in determining the biological effect of an energetic particle, then *LET* may not be the best parameter for characterizing the particle track. The quantity  $z^{*2}/\beta^2$  (where  $z^*$  is the effective charge and  $\beta$  is the relative velocity) has been suggested as a more relevant alternative (Katz 1970) as the energy deposited by the secondary electrons of particles matched using this parameter are similar. It can be shown that our data supports the notion that  $z^{*2}/\beta^2$  is a relevant parameter by noting that our data indicate peak effectiveness of about 55–60 and 95 keV  $\mu\text{m}^{-1}$  for singly and doubly charged ions respectively, and that the corresponding value of  $z^{*2}/\beta^2$  for both of these is about 1660. The conclusion that can be drawn from this is that the *RBE* of a charged-particle is not simply a function of the ionization density along the track, but also depends on the radial dose-distribution around the track. However, although the use of  $z^{*2}/\beta^2$  brings the peaks into approximate alignment, the peak *RBEs* appear to differ and are therefore not determined by the value of  $z^{*2}/\beta^2$ .

#### 4. Conclusions

In agreement with our previous work, and that of other workers, our data suggest that the *RBE* for cell survival of V79 cells exposed to singly-charged particles is greater than that for helium ions of the same *LET* at moderate *LET* values (i.e. about 40–50 keV  $\mu\text{m}^{-1}$ ). We have also shown that deuterons have a similar *RBE* to protons with the same *LET*, and that we can exploit the greater range of deuterons to extend the measurements to higher *LET* than are possible using only protons. Our data show that the *RBE* for protons and deuterons

increases with increasing *LET* up to the highest *LET* used (50 keV  $\mu\text{m}^{-1}$ ), and suggest that the peak *RBE* might be about 55–65 keV  $\mu\text{m}^{-1}$ . Finally, we have shown that the differences between *LET*-matched singly and doubly charged particles can be understood in terms of the differences in radial dose distribution around the primary ion track.

#### Acknowledgements

This work is supported by the Cancer Research Campaign and by grants from the Radiation Protection Research Action Programme of the European Community. We should also like to thank the staff of the Gray Laboratory mechanical and electrical workshops.

#### References

- BELLI, M., CHERUBINI, R., FINOTTO, S., MOSCHINI, G., SAPORA, O., SIMONE, G. and TABOCCHINI, M. A., 1989, RBE-LET relationship for the survival of V79 cells irradiated with low energy protons. *International Journal of Radiation Biology*, **55**, 93–104.
- BELLI, M., CERA, F., CHERUBINI, R., IANZINI, F., MOSCHINI, G., SAPORA, O., SIMONE, G., TABOCCHINI, M. A. and TIVERON, P., 1992b, RBE-LET relationship for survival and mutation induction of V79 cells irradiated with low-energy protons: re-evaluation of the LET values at the LNL facility. *International Journal of Radiation Biology*, **61**, 145–146.
- BELLI, M., CERA, F., CHERUBINI, R., HAQUE, A. M. I., IANZINI, F., MOSCHINI, G., SAPORA, O., SIMONE, G., TABOCCHINI, M. A. and TIVERON, P., 1993, Inactivation and mutation induction of V79 cells by low-energy protons: re-evaluation of the results at the LNL facility. *International Journal of Radiation Biology*, **63**, 331–337.
- BELLI, M., CERA, F., CHERUBINI, R., GOODHEAD, D. T., HAQUE, A. M. I., IANZINI, F., MOSCHINI, G., NIKJOO, H., SAPORA, O., SIMONE, G., STEVENS, D. L., TABOCCHINI, M. A. and TIVERON, P., 1994, Inactivation induced by deuterons of various LETs in V79 cells. *Radiation Protection Dosimetry*, **52**, 305–310.
- BELLI, M., GOODHEAD, D. T., IANZINI, F., SIMONE, G. and TABOCCHINI, M. A., 1992a, Direct comparison of biological effectiveness of protons and  $\alpha$ -particles of the same LET. II. Mutation induction at the HPRT locus in V79 cells. *International Journal of Radiation Biology*, **61**, 625–629.
- CHERUBINI, R., CERA, F., HAQUE, A. M. I., TIVERON, P., MOSCHINI, G., SIMONE, G., BELLI, M., IANZINI, F., SAPORA, O. and TABOCCHINI, M. A., 1993, Mutation induction of low energy protons in V79 cells. Abstracts of papers for the 41st Annual Meeting of the Radiation Research Society and the 13th Annual Meeting of the North American Hyperthermia Society, Dallas, Texas, 135.
- DATTA, R., COLE, A. and ROBINSON, S., 1976, Use of track-end alpha particles from  $^{241}\text{Am}$  to study radiosensitive sites in CHO cells. *Radiation Research*, **65**, 139–151.

- FOLKARD, M., PRISE, K. M., VOJNOVIC, B., DAVIES, S., ROPER, M. J. and MICHAEL, B. D., 1989, The irradiation of V79 Mammalian cells by protons with energies below 2 MeV. Part I: Experimental arrangement and measurement of cell survival. *International Journal of Radiation Biology*, **56**, 221–237.
- FOLKARD, M., PRISE, K. M., VOJNOVIC, B., NEWMAN, H. C., ROPER, M. J., HOLLIS, K. J. and MICHAEL, B. D., 1995, Conventional and microbeam studies using low-energy charged particles relevant to risk assessment and the mechanisms of radiation action. *Radiation Protection Dosimetry*, **61**, 215–218.
- FRANKENBERG, D., GOODHEAD, D. T., FRANKENBERG-SCHWAGER, M., HARBICH, R., BANCE, D. A. and WILKINSON, R. E., 1986, Effectiveness of 1.5 keV aluminium K and 0.3 keV carbon K characteristic X-rays at inducing DNA double-strand breaks in yeast cells. *International Journal of Radiation Biology*, **50**, 727–741.
- GOODHEAD, D. T., BELLI, M., MILL, A. J., BANCE, D. A., ALLEN, L. A., HALL, S. C., IANZINI, F., SIMONE, G., STEVENS, D. L., STRETCH, A., TABOCCHINI, M. A. and WILKINSON, R. E., 1992, Direct comparison of biological effectiveness of protons and  $\alpha$ -particles of the same LET. I. Irradiation methods and inactivation of asynchronous V79, HeLa and C3H 10T1/2 cells. *International Journal of Radiation Biology*, **61**, 611–624.
- GOODHEAD, D. T., 1994, Initial events in the cellular effects of ionizing radiations: clustered damage in DNA. *International Journal of Radiation Biology*, **65**, 7–17.
- ICRU, 1993, *Stopping Powers and Ranges for Protons and  $\alpha$ -Particles*. Report 49 (Washington: International Commission on Radiation Units and Measurements).
- KATZ, R., 1970, RBE, LET and  $Z^{*2}/\beta^2$ . *Health Physics*, **18**, 175.
- PERRIS, A., PIALOGLU, A. A., KATSANOS, A. A. and SIDERIS, E. G., 1986, Biological effectiveness of low energy protons. I. Survival of Chinese hamster cells. *International Journal of Radiation Biology*, **50**, 1093–1101.
- PRISE, K. M., FOLKARD, M., DAVIES, S. and MICHAEL, B. D., 1990, The irradiation of V79 Mammalian cells by protons with energies below 2 MeV. Part II: Measurement of oxygen enhancement ratios and DNA damage. *International Journal of Radiation Biology*, **58**, 261–277.
- RAJU, M. R., 1995, Proton radiobiology, radiosurgery and radiotherapy. *International Journal of Radiation Biology*, **67**, 237–259.
- THACKER, J., STRETCH, A. and STEPHENS, M. A., 1979, Mutation and inactivation of cultured mammalian cells exposed to beams of accelerated heavy ions. II. Chinese hamster V79 cells. *International Journal of Radiation Biology*, **36**, 137–148.
- THACKER, J., WILKINSON, R. E. and GOODHEAD, D. T., 1986, The induction of chromosome aberrations by carbon ultra-soft X-rays in V79 hamster cells. *International Journal of Radiation Biology*, **49**, 645–656.